

**Introduction:** Removal of atmospheric dust effects is required to derive surface IR spectral emissivity. Atmospherically corrected emissivities will allow us to constrain the physical properties of the polar cap. Commonly, the atmospheric-surface separation is based on radiative transfer (RT) spectral inversion methods using nadir-pointing observations [1,2]. This methodology depends on a priori knowledge of the spectral shape of each atmospheric aerosol (e.g. dust or water ice) and a large thermal contrast between the surface and atmosphere. RT methods commonly fail over the polar caps due to low thermal contrast between the atmosphere and the surface.

**Data:** We have used multi-angle Emission Phase Function (EPF) observations to estimate the opacity spectrum of atmospheric dust over the springtime south polar cap and the underlying surface radiance, and thus, the surface emissivity. We include an EPF from Hellas Basin as a basis for comparison between the spectral shape of polar and non-polar dust. Surface spectral emissivities over the seasonal cap are compared to CO<sub>2</sub> models.

#### Analysis:

*Algorithm.* The algorithm used is based on radiative transfer code, as outlined by Smith et al.[1] and Bandfield et al.[3].

$$I_\nu = \epsilon_\nu \beta_\nu(T_{\text{surf}}) e^{-\tau_0/\mu} + \frac{\tau_0}{P_0 \mu} \int_0^{P_0} \beta_\nu(T(P)) e^{-\frac{\tau_0}{P_0 \mu} P} dP$$

where  $I_\nu$  is the observed radiance,  $\epsilon_\nu$  is the wavenumber dependent emissivity,  $T_{\text{surf}}$  is the surface temperature,  $\tau_0$  is the wavenumber dependent atmospheric opacity,  $1/\mu$  is the airmass,  $P_0$  is the surface pressure, and  $T(P)$  is the atmospheric temperature profile.

Since each observation in an EPF has a derived atmospheric temperature profile [4], we use the mean  $T(P)$ , as well as the mean of the surface pressure and the mean of the surface temperature. We use a best-fit method where there are no constraints on the value of  $\epsilon_\nu$  or  $\tau_0$ . Because we allow  $\epsilon_\nu$  to be greater than unity, we can measure the accuracy of the surface temperature, and adjust the emissivity accordingly.

*Limitations.* The current implementation assumes that the atmosphere has no large lateral thermal or opacity gradients. This assumption is not valid near the edge of the polar cap. We also assume that the thermal properties of the surface are generally homogeneous and the elevation change is small over the spatial extent of the observations. Bandfield and Smith [3] used this same methodology to analyze southern equatorial EPFs. They removed the effects of CO<sub>2</sub> hot bands and H<sub>2</sub>O vapor prior to doing the EPF analysis; we do neither. The methods to derive the CO<sub>2</sub> hot bands and H<sub>2</sub>O vapor radiance contributions

are unreliable under the surface and atmospheric temperature conditions found at the springtime south polar cap. Therefore, we assume that all effects from the atmosphere are well mixed and we apply the EPF analysis to the uncorrected spectra.

*CO<sub>2</sub> Spectral Models:* To assist in the analysis of derived surface emissivity, the reflectance and emissivity of deposits of CO<sub>2</sub> frost, with mixtures of small amounts of dust, were calculated using the CO<sub>2</sub> complex refractive indices of Hansen [5], and the methodology described in Kieffer et al. [6].

**Atmospheric Results:** Our results show that the spectral shape of the polar dust opacity is not constant, but is a two-parameter family that can be characterized by the 9  $\mu\text{m}$  and 20  $\mu\text{m}$  opacities [Fig. 1]. The 9  $\mu\text{m}$  opacity varies from 0.15 to 0.45 and characterizes the overall atmospheric conditions [Fig. 2]. The 9  $\mu\text{m}$  to 20  $\mu\text{m}$  opacity ratio varies from 1.9 to 5.6, suggesting that atmospheric polar dust either changes in dust size distribution or is coated, perhaps by H<sub>2</sub>O ice [Fig. 3].

Dust opacity is generally enhanced over the cryptic region. This is generally consistent with greater sublimation winds over the region and supports the self-cleaning mechanism proposed by Kieffer et al.[4].

The 9  $\mu\text{m}$  to 20  $\mu\text{m}$  opacity ratio seems more correlated with seasonal trends than with location. The greatest ratio occurs in early spring and late spring, just prior to exposure of soil. The lowest ratio (most like the Hellas dust) occurs at L<sub>s</sub> 220° - 235°.

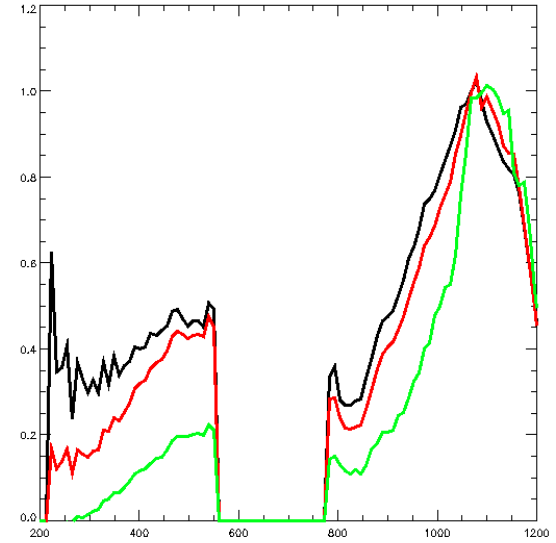


**Figure 1: Atmospheric Endmember Spectra.** The black line is an example of the dust opacity over Hellas basin. The red line is the mean dust opacity of three polar EPFs that are closest in shape to the Hellas EPF. The green line is the mean dust opacity of 2 polar EPFs that are the most different from the Hellas EPF.

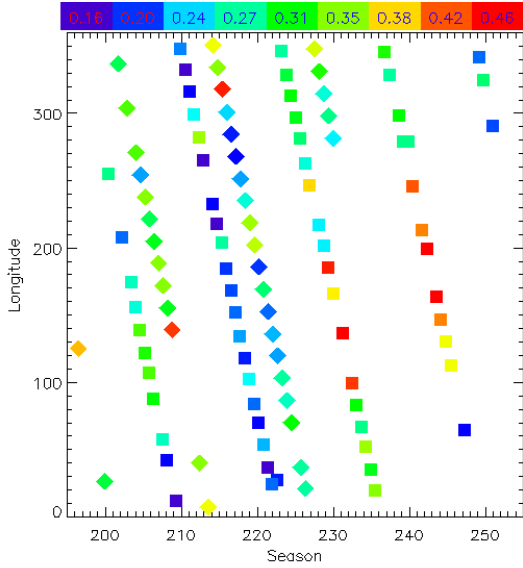


**Figure 2: 9um opacity distribution.** Boxes are EPFs at 85°S and diamonds are EPFs from 75°S. The highest dust opacity is spacially correlated with the cryptic region.

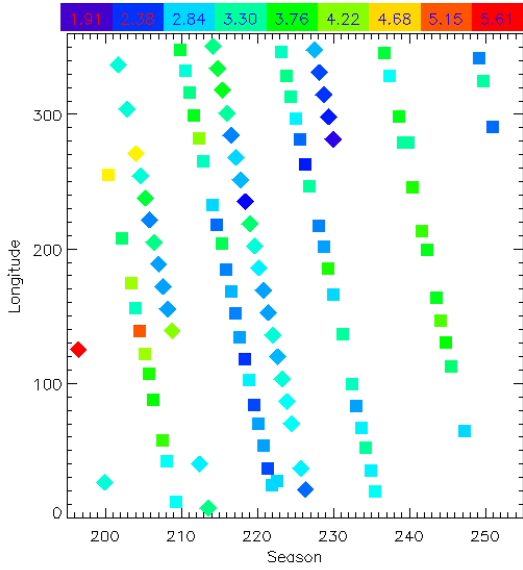


**Figure 3: 9 um to 20 um opacity ratio distribution.** The appears to be little spatial correlation. The dust is most similar to the Hellas EPF when the 9  $\mu\text{m}$  to 20  $\mu\text{m}$  ratio is lowest, from  $L_s$  220°-235°.

**Surface Results:** We derived the surface temperature from each radiance spectrum by assuming that the surface temperature was the highest brightness temperature in the spectral range of  $222 \text{ cm}^{-1}$  and  $550 \text{ cm}^{-1}$ . This temperature was compared to the calculated  $\text{CO}_2$  frost temperature. The derived surface temperatures from the EPFs confirm that the slightly elevated temperatures (relative to  $\text{CO}_2$  frost temperature) observed in "cryptic" regions are a surface effect, not atmospheric [Fig. 4]. It is unlikely

the elevated surface temperatures are due to partial defrosting since the surface remains cold for several sols after the elevated temperatures occur. Perhaps the elevated temperatures are due to near surface effects of hot dust, where the dust is not in thermal contact with the surface ice.

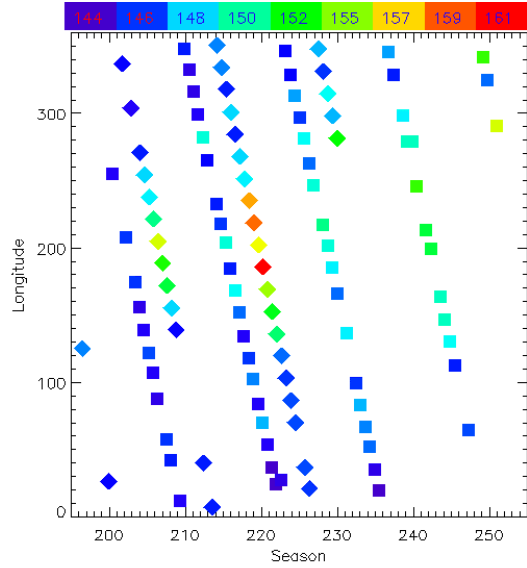


**Figure 4: Surface Temperature.** The EPF-derived surface temperature is consistent with solid  $\text{CO}_2$ , except for the cryptic region around  $L_s$  225°. Since the temperatures do not increase, but actually decrease, solid  $\text{CO}_2$  must still be present.

Comparison of broad-band reflectivity and surface emissivities to model spectra suggest the bright regions (e.g., perennial cap, Mountains of Mitchell) have higher albedos due to either a thin surface layer of fine-grain  $\text{CO}_2$  (perhaps either frost or fractured ice) with an underlying layer of either coarse grain or slab  $\text{CO}_2$  ice or a small amount of  $\text{H}_2\text{O}$  ice. Observations of layering of  $\text{CO}_2$  ice and frost is consistent with results from an EPF analysis of Mariner 7 spectra done by Calvin [7]. We still do not understand why the "cryptic" region remains monolithic throughout the spring while the rest of the cap becomes layered.

#### References:

- [1] Smith, M. D. et al. (2000) *JGR*, **105**, 9589-9608.
- [2] Bandfield, J. L. et al. (2000) *JGR*, **105**, 9573-9588.
- [3] Bandfield, J. L. and Smith, M. D. (2001) *LPS XXXIII*, 1596.
- [4] Conrath, B. J. et al. (2000) *JGR*, **102**, 9509-9520.
- [5] Hansen, G. B. (1997) *JGR*, **105**, 21569-21587.
- [6] Kieffer, H. H. et al. (2000) *JGR*, **105**, 9653-9699.
- [7] Calvin, W. M. and Martin, T. Z. (1994) *JGR*, **105**, 21143-21152.

